Exploring Feature Coupling for Multiple Operations Type and Order Detection

Shangde Gao, Jiaxin Chen*, Xin Liao
College of Computer Science and Electronic Engineering, Hunan University, Changsha 410082, China

2022 IEEE 24th International Workshop on Multimedia Signal Processing (MMSP) | 978-1-6654-7189-3/22/$31.00 ©2022 IEEE | DOI: 10.1109/MMSP55362.2022.9948960

***Abstract*—To assess the authenticity and integrity of digital image history, forensic analysts not only need to identify the types of tampering operations that multimedia has undergone but also distinguish their topological combination order. However, due to the interaction among tampering operations, a forensic method proposed for the operation identification yields unacceptably low performance when the content of a given image was forged by operations in a multi-operator chain. In this paper, we propose an efficient detection framework for determining the type and order of the tampering operations. Specifically, we first divide the operation detection problem into two aspects: operation type identification and their combination order detection. Then, by exploring the feature coupling relationships among different features with Pearson's correlation coefficient, optimal coupled features are designed for tampering operations detection. Finally, the detection of multiple operations applied to the previously JPEG-compression images is examined, and the effectiveness of our proposed framework has been demonstrated by simulation results.**

***Index Terms*—Image forensics, operator chains detection, coupled feature, feature coupling matrix**

I. Introduction

With the rapid development of image editing software, digital images can be easily manipulated and falsified. To verify the authenticity and integrality of digital contents, image forensics has emerged as an important research field [1]. Recently, many state-of-the-art forensic techniques have been proposed to identify the use of different manipulation operations, such as resampling [2], [3], contrast enhancement [4], [5], and median filtering [6], [7]. Furthermore, some universal forensic techniques [8] have been proposed for various types of tampering operations identification.

Multiple manipulation operations, however, may be used to create a forgery in real scenarios. In this vein, Chen et al. [9] proposed a features decoupling method to identify multiple tampering operations in different operator chains. A decision fusion method [10] was designed to integrate multiple forensic knowledge and improve the operations detection performance in image operator chains. Besides identifying the existence of each tampering operation, it is even more crucial to detect the order of operations applied. In [11], Stamm et al. focused on a scenario where the image was manipulated by contrast enhancement and resizing. A conditional fingerprint was proposed to distinguish their tampering order. In [12], Chu et al. formulated the order detection problem as a multi-hypotheses test problem. Then, an information theoretical framework was proposed to model the relationship between the detected hypothesis and the true hypothesis. Besides, conditional fingerprints were designed to measure the order of certain binary operator chains. Liao et al. [13] proposed a two-stream convolutional neural network to detect image operator chains, which can capture both tampering trace evidence and local noise residual evidence.

Nevertheless, because of the coupling artifacts among tampering operations (i.e., subsequent tampering operations can weaken or even erase the traces of previous ones), it is difficult to construct a suitable conditional fingerprint to directly discriminate the operations type and topological order in multi-operator chains.

In this paper, we present a detection framework for forensically determining the type and order in which a set of processing operations have been applied to forge images. To accomplish this, we first formulate the type and order of multiple processing operations detection as two multiple hypothesis testing problems. Pearson's correlation coefficient is used to exploit the coupling relationships between different operation pairs. Meanwhile, coupled features are investigated to differentiate these hypotheses. In our experiments, we demonstrate the effectiveness of our detection framework by using it to examine the pre-JPEG images which may have been manipulated with contrast enhancement, up-sampling, and median filtering.

II. Type and Order of Operations Detection Framework

To determine the tampering operations type and order in multiple operator chains, we first formulate them as two multi-hypotheses testing problems. Then, considering various features that characterize the fingerprints of different tampering operations from diverse views. By exploring the coupling relationships among these features, coupled features are generated for tampering operations type and order detection. As shown in Fig. 1, the detailed presentation of the detection framework is as follows.

1) *Original Feature Representation*. The original features of the images in the image collection are extracted.

2) *Coupled Feature Representation*. After mining feature coupling relationships, reconstruct original features to generate coupled features.

*Corresponding author:
Email address: chenjiaxin@hnu.edu.cn (Jiaxin Chen)

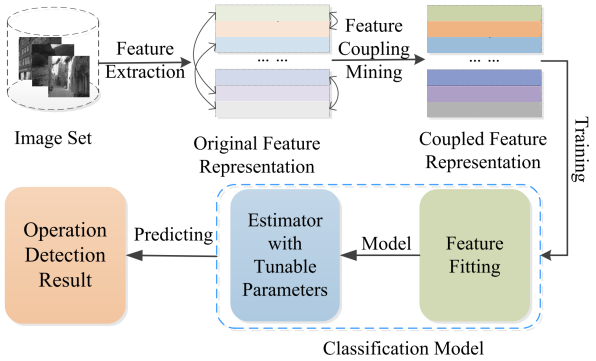

Fig. 1. The framework for detecting tampering operations in multiple operator chains.

3) *Classification Model*. Based on designed multi-hypotheses, modeling the distribution of coupled feature contents with a multi-class classifier, and developing certain detectors with tunable parameters to contrast information entropy between the true and detected hypotheses.

According to the above detection framework, three main problems, namely, the identification of multiple operations, the distinction in the topological order of operations, and feature reconstruction based on the coupling feature relationships, can be solved. The detailed process is elaborated in the following subsections.

A. Specific Operation Type Identification

To identify the existence of each operation in multiple operator chains, we need to separate the considered multiple operator chains into binary chains set. One set contains the topologies detected operation, the other does not. We can formulate the operation separation problem as a hypothesis testing problem. Let $O = (O_1, O_2, \ldots, O_m)$ denote the considered manipulation operations, towards any operation $O_i (i = 1, 2, \ldots, m)$, the possible identification result of a questionable image must be the following binary hypothesis testing problem.

$$H_0 : \text{It contains the tampering operation } O_i,$$
$$H_1 : \text{It does not contain the tampering operation } O_i.$$

where H_0 and H_1 are the considered hypotheses, they are oppositive to each other. The true and detected hypothesis, denoted as H and $\hat{H}$ respectively, belong to those hypotheses.

To contrast the entropy between H and $\hat{H}$, *prior information* is first calculated as,

$$P_{prior} = \frac{\sum_{i=1}^{m} C_i^1 A_{m-1}^{i-1}}{\sum_{j=1}^{m} A_m^j} \tag{1}$$

where A and C are symbols of permutation and combination. The denominator represents the considered number of multiple operator chains, and the numerator represents the number of multiple operator chains containing O_i.

For the given multimedia content, after modeling the distribution of its coupled feature with a specific detector $d_{\underline{\theta}}$, the type of O_i can be identified if H and $\hat{H}$ satisfy the following discriminant criterion,

$$P_{\underline{\theta}}(\hat{H} = \hat{H}_j | H = \hat{H}_j) > P_{prior} + \epsilon_1, \quad j = 0, 1 \tag{2}$$

where $\underline{\theta}$ denotes the tunable parameters of detector d, $\epsilon_1 \geq 0$ is the confidence factor indicating how well the hypothesis can be distinguished from others.

B. Topological Order Detection

Assuming that after the process of identifying tampering operations type in Section II-A, there remain n tampering operations, denoted as $O = (O_1, O_2, \ldots, O_n)$, $n \leq m$. To further distinguish their topological order, $S = (S_1, S_2, \ldots, S_v)$ is preliminary used to denote the full permutation results of those tampering operations, where $v = A_n^n$. Given the topological tampering operator chains S_i and S_j, $i \neq j$, we aim to determine whether the given image content is tampered by S_i or S_j. Therefore, the topological order detection problem can be formulated as a multiple hypotheses testing problem in the following.

$$H_i : \text{It is altered by the tampering operator chains } S_i,$$
$$H_j : \text{It is altered by the tampering operator chains } S_j.$$

where H_i and H_j are mutually exclusive to each other.

Before contrasting these hypotheses, the first step is to determine whether there exist coupling relationships between S_i and S_j. Denote the tampered image that experienced S_i and S_j as I_i and I_j, respectively. If they are uncoupled, the tampered image contents must be the same, i.e., $I_i = I_j$, thus they can't distinguish from each other. Otherwise, S_i and S_j are coupled with each other. In this vein, coupled features can be designed to extract those unique fingerprints in I_i and I_j to distinguish their order.

Then, as for any two coupled operator chains S_i and S_j, via modeling the distributions of their coupled features, certain detector $d_{\underline{\theta}}$, can be developed to contrast their detecting hypotheses H_i and H_j. The topological order of S_i and S_j can be distinguished if the transition probability between H and $\hat{H}$ satisfies the following discriminant criterion,

$$P_{\underline{\theta}}(\hat{H} = H_i | H = H_i) > P_{\underline{\theta}}(\hat{H} = H_j | H = H_i) + \epsilon_2, \tag{3}$$

where $\epsilon_2 \geq 0$ are confidence factors indicating how well the hypothesis can be distinguished from others.

C. Coupling Feature Measure

In [14], the research on image source identification have mentioned that various features characterize the fingerprints from different views, therefore they are naturally coupled to each other. In this vein, their coupling relationships can be measured by Pearson's correlation coefficient.

TABLE I
ORIGINAL FEATURES REPRESENTATION OF DIFFERENT DETECTION METHODS.

Type	Original Features	Dimension	Alias
CE	Frequency energy metric [4]	1×1	f^1_{CE}
	Zero-height gap bins [5]	1×1	f^2_{CE}
US	Normalized energy density [3]	1×18	f^1_{US}
	Frequency pmap bins	1×18	f^2_{US}
MF	Residual groups [7]	1×7	f^1_{MF}
	2nd-order LTP	1×16	f^2_{MF}

Given the feature f^x_i and f^y_j, the image set Φ, Pearson's correlation coefficient of f^x_i and f^y_j can be calculated as,

$$Cor(f^x_i, f^y_j) = \frac{\sum_{I\in\Phi}(f^x_i(I) - \bar{f^x_i})(f_j(I) - \bar{f^y_j})}{\sqrt{\sum_{I\in\Phi}(f^x_i(I) - \bar{f^x_i})^2}\sqrt{\sum_{I\in\Phi}(f^y_j(I) - \bar{f^y_j})^2}} \tag{4}$$

where I is an image in Φ, $f^x_i(I)$ denotes the feature value of I on f^x_i. $\bar{f^x_i}$ represents the mean value of f^x_i on Φ. Further, the coupling gains (CG) of f^y_j to f^x_i can be described as,

$$CG(f^x_i|f^y_j) = w^{x,y}_{i,j} \cdot f^y_j \tag{5}$$

where $w^{x,y}_{i,j} = Cor(f^x_i, f^y_j)$. If f^x_i and f^y_j are positively correlated, they would have positive gains for each other. Otherwise, if they are negatively correlated, the gains are negative.

Suppose the feature set is $F = (f^1_1, f^2_1, \ldots, f^{u-1}_m, f^u_m)$, the pairwise coupling relationships of features in F can be represented as Feature Coupling Matrix (FCM).

$$FCM = \begin{pmatrix} Cor(f^1_1, f^1_1) & Cor(f^1_1, f^2_1) & \cdots & Cor(f^1_1, f^u_m) \\ Cor(f^2_1, f^1_1) & Cor(f^2_1, f^2_1) & \cdots & Cor(f^2_1, f^u_m) \\ \vdots & \vdots & \ddots & \vdots \\ Cor(f^u_m, f^1_1) & Cor(f^u_m, f^2_1) & \cdots & Cor(f^u_m, f^u_m) \end{pmatrix} \tag{6}$$

Based on the obtained FCM, different features can concatenate with each other to generate new coupled features (CR) $\tilde{F}$, denoted as $\tilde{F} = (\tilde{f^1_1}, \tilde{f^2_1}, \ldots, \tilde{f^{u-1}_m}, \tilde{f^u_m})$. For example, the coupled feature $\bar{f^x_i}$ can be represented as,

$$\bar{f^x_i} = f^x_i + CG(f^x_i|F_{-f^x_i}) = f^x_i + \mathbf{W}^x_i \cdot (F_{-f^x_i}), \tag{7}$$

where $F_{-f^x_i} = F - \{f^x_i\} = (f^1_1, \ldots, f^{x-1}_i, f^{x+1}_i, \ldots, f^u_m)$. $\mathbf{W}^x_i$ is the extended weight vector, which can be represented as $\mathbf{W}^x_i = (w^{x,1}_{i,1}, \ldots, w^{x,y}_{i,j}, \ldots, w^{x,u}_{i,m})$.

Then, combined with the designed discriminant criterion above subsections, the confusion probability matrix is generated to evaluate the effectiveness of our detection framework.

III. EXPERIMENTS OF OPERATOR CHAINS DETECTION IN MULTIPLE OPERATOR CHAINS

We demonstrate the effectiveness of the proposed detection framework on a list of benchmark, and provide implementation details, comparative results and discussions, as follows.

TABLE II
AVERAGE DETECTION ACCURACIES (%) FOR IDENTIFYING THE TYPES OF TAMPERING OPERATIONS WITH DIFFERENT ORIGINAL AND COUPLED FEATURES.

Features		UNAT	CE	US	MF
Original	f^1_{CE}	50.00	*75.00*	51.15	50.00
	f^2_{CE}	50.00	50.00	86.65	50.00
	f^1_{US}	*59.00*	50.00	62.40	88.90
	f^2_{US}	50.00	50.00	63.65	52.55
	f^1_{MF}	65.35	50.00	83.80	88.00
	f^2_{MF}	56.05	57.40	*89.35*	*95.70*
Coupled	$\tilde{f^1_{CE}}$	94.45	92.15	97.40	98.00
	$\tilde{f^2_{CE}}$	94.45	92.15	97.40	98.00
	$\tilde{f^1_{US}}$	98.00	90.05	97.75	99.35
	$\tilde{f^2_{US}}$	95.50	90.95	97.45	99.20
	$\tilde{f^1_{MF}}$	92.10	91.95	97.40	97.15
	$\tilde{f^2_{MF}}$	96.50	91.95	97.45	99.25

A. Experiments Setup

a) Datasets: Our detection framework is evaluted on two widely used benchmarks, i.e, BOSS [15] and UCID [16]. First, we previously pressed input images with different qualification factors (QF=75, 80, 85, 90). Then, each image is center cropped to 256×256 for fair comparison. We employ 1K BOSS for training the SVM, 800 images from overall 1338 UCID images are used for testing.

b) Implementation details: We implement our method using SVM on CPUs of Intel® Xeon® Gold 6139 CPU @ 2.30GHz. $(0, 1)$ uniform distribution is utilized to initialize the extended weights $\mathbf{W}$ in section II-C. We use RBF-kernel with its default settings to train the SVM.

B. Original and Coupled Features Representation

In this experiment, we give an example to determine the state-of-art original and coupled features, used for detecting the types of tampering operations in multiple operator chains.

To obtain the original features, we extract 6 state-of-art feature sets from three different single operations detection methods [3]–[7], denoted as $F = (f^1_{CE}, f^2_{CE}, \ldots, f^2_{MF})$. Among them, we propose a new up-sampling detection method (f^2_{US}) and reduce the feature dimensions of f^2_{MF}. Table I summaries all types of considered tampering operations, the dimensions and aliases of original features.

In the process of acquiring coupled features, according to Eq. (4), the dimensions must be the same between any two feature sets. Therefore, each feature set in Table I is extended to an 18-D (dimensions) vector to calculate the correlation coefficient. Specifically, by self-replication, extend f^1_{CE} and f^2_{CE} to 18 dimensions. After concatenating f^1_{MF} with its mean and variance values, extend the result to an 18-D vector by self-replication.

TABLE III
COMPARISON DETECTION RESULTS (%) FOR IDENTIFYING THE TYPES OF OPERATIONS USING THE STATE-OF-ART ORIGINAL FEATURES, LI ET AL. [8], AND OUR COUPLED FEATURES.

Tunable Parameters		UNAT			CE			US			MF		
QF	β	Li [8]	Original	Our	Li [8]	Original	Our	Li [8]	Original	Our	Li [8]	Original	Our
QF = 90	β_1	98.70	67.30	**98.00**	50.00	58.05	**93.05**	97.92	86.15	**97.45**	99.50	95.70	**99.45**
	β_2	95.80	55.55	**98.20**	50.00	54.00	**87.05**	98.35	87.05	**96.50**	99.90	93.50	**99.25**
QF = 85	β_1	98.80	69.90	**97.45**	50.00	55.90	**92.15**	98.10	86.70	**97.65**	99.75	95.00	**99.45**
	β_2	96.35	62.55	**97.20**	50.00	53.55	**87.40**	98.45	87.00	**96.35**	99.90	91.50	**99.10**
QF = 80	β_1	98.55	71.05	**97.65**	50.00	59.50	**91.55**	98.35	86.70	**97.65**	99.70	93.95	**99.40**
	β_2	96.55	65.80	**97.20**	50.00	52.85	**87.25**	98.50	87.05	**96.30**	99.80	91.00	**99.22**
QF = 75	β_1	98.70	71.05	**97.65**	50.00	56.75	**90.50**	98.70	86.65	**97.55**	99.90	93.50	**99.45**
	β_2	100.00	64.18	**97.00**	50.00	52.65	**87.50**	98.45	87.00	**96.50**	99.80	91.50	**99.25**

Following the coupling feature measure method proposed in Section II-C, the absolute result of FCM is integrated by Pearson's correlation coefficient as follows.

$$FCM = \begin{pmatrix} 1 & 1 & 0.22 & 0.25 & 0.74 & 0.75 \\ 1 & 1 & 0.22 & 0.25 & 0.74 & 0.75 \\ 0.22 & 0.22 & 1 & 0.49 & 0.95 & 0.52 \\ 0.25 & 0.25 & 0.49 & 1 & 0.75 & 0.12 \\ 0.74 & 0.74 & 0.95 & 0.75 & 1 & 0.96 \\ 0.75 & 0.75 & 0.52 & 0.12 & 0.96 & 1 \end{pmatrix}. \quad (8)$$

Then, the obtained coupled features can be denoted as $\tilde{F} = (f^{\tilde{1}}_{CE}, f^{\tilde{2}}_{CE}, \ldots, f^{\tilde{2}}_{MF})$. To verify the detection performance of different elements in F and $\tilde{F}$, 1000×16 images and 800×16 images are generated for training and testing, where $QF = 90$, the tunable parameters group of gamma coefficient, sampling factor, and windows filter (with corresponding to CE, US, MF) are $\beta = (1.2, 1.25, 3 \times 3)$.

The detection results are shown in Table II. By minimizing the average decision error P_e between the false-positive rate and given the false-negative rate of each element, the original and coupled features, marked as italics and underline, have been discovered for identifying whether a test image is unaltered (UNAT) or altered by above tampering operations.

C. Specific Operation Identification Experiments

In this experiment, we try to identify the type of image processing operation previously used for a given questionable image. In our experiments, all types of image operations listed in Table I are considered, i.e., $O = (O_1, O_2, O_3)$, $m = 3$.

For each original image, we created 16 counterparts using a random parameter for each operation. To evaluate the effectiveness of the proposed detection framework, we tested the detection performance of our coupled features in Table II. Besides, the universal forensic feature Li [8] and four original features listed in Table II without using our detection framework were included for comparative studies.

The average detection accuracies are shown in Table III, where the random parameter groups are $\beta_1 = (0.7, 1.5, 5 \times 5)$, $\beta_2 = (1.2, 1.25, 3 \times 3)$. Followed the discriminant criterion in II-A, it is observed that the questionable images altered by the operator chain containing CE can not be correctly identified with f^{1}_{CE} and Li [8]. The main reason is that the test image has not been forged by the operation CE was misjudged as containing CE. Compared to Li [8] and state-of-art original features, our coupled features based on a detection framework are very useful and robust for identifying various types of tampering operations in multi-operator chains.

TABLE IV
ORDER DETECTION ACCURACIES (%) OF CONTRAST ENHANCEMENT AND UP-SAMPLING WITH CHU ET AL. [12] AND THE OPTIMAL COUPLED FEATURE.

QF	CE-US		US-CE	
	Chu [12]	Our	Chu [12]	Our
QF = 90	81.70	**99.60**	79.94	**97.00**
QF = 85	79.87	**99.80**	79.75	**97.80**
QF = 80	79.12	**99.90**	78.80	**98.50**
QF = 75	78.87	**99.90**	77.40	**98.50**

D. Topological Order Detection Experiments

Assuming that there are 2 tampering operations after the process of operation type identification, i.e., $O = (O_1, O_2)$, and $n = 2$. Thus, three possible combination cases should be considered, i.e., contrast enhancement and up-sampling, contrast enhancement and median filtering, median filtering and up-sampling.

Based on the coupling relationships discriminant criterion investigated in Section II-B, it is known that the image contents are tampered by the contrast enhancement then median filtering (CE-MF), and median filtering then contrast enhancement (MF-CE) are the same. Thus, they are uncoupled and can not distinguish between each other.

Contrast enhancement and resizing are coupled with each other, the coupled features for topological order detection can be presented as $\tilde{F} = (f^{\tilde{1}}_{CE}, f^{\tilde{2}}_{CE}, f^{\tilde{1}}_{RS}, f^{\tilde{2}}_{RS})$. To verify the effectiveness of our detection framework, the optimal feature $f^{\tilde{2}}_{RS}$ was used to distinguish their tampering order, and the detection method in [12] without using our framework

was included for comparative investigation. The experimental detection comparison results are presented in Table IV, where the gamma coefficient and scale factor are 0.7 and 1.5, respectively.

Compared with the detection method in [12], our coupled feature can efficiently distinguish the tampering order of contrast enhancement and up-sampling.

E. Discussion

In this section, we first visualize two different re-weighted FCMs produced on the detecting tasks of UCID dataset in Figure 6, then enumerate the weakness of current framework to provide direction for future work.

c) Visualization: The blue heatmaps summarize the re-weighted FCMs (7), averaged across several features for each detecting operation. Specifically, the element on each grid is the re-weighted Pearson's correlation coefficient computed on testing set. We found that the uniform strategy (left) learns relatively smoother weight distributions that blends different features, while the filtered one (right) consistently puts most of its weight on the on the features extracted from the same task.

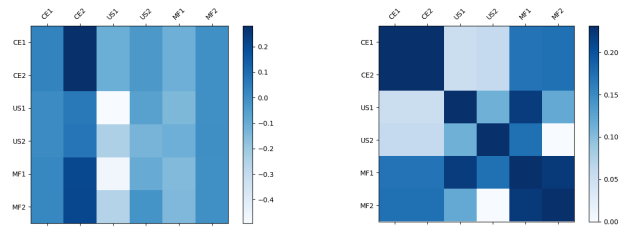

(a) Re-weighted FCM with the $(0, 1)$ uniform weights

(b) Re-weighted FCM with the filterd weights (filter the coefficient ≤ 0.15)

Fig. 6. Visualization of Feature Coupling Matrix (FCM) with two different re-weighted strategies. Rows and columns correspond to the extracted features of the detecting tasks.

d) Limitations: Our detection framework suffers from few problems as follows. First, it is difficult to unify d-ifferent benchmarks, because their feature dimensions are different. Secondly, the fixed weighting strategy restricts the adaptive representation of coupled features, leading to sub-optimization. Our future work will focus on knowledge fusion strategy and attention-based adaptive weighting.

IV. Conclusion

In this paper, we investigate the fundamental question of how to detect tampering operations in multiple operator chains. To answer this question, we formulate the operation detection problem into two hypotheses testing problems. Then, via mining the coupling feature measure and reconstructing coupled features, a detection framework is proposed to answer how to detect the type and order of tampering operations. For the case study, based on the pre-JPEG compression images, we examine the problem of identifying the operation types and detecting their topological order in certain multi-operator chains. Simulations show that our proposed framework is useful and efficient.

Acknowledgment

This work is partially supported by the National Natural Science Foundation of China (Grant No. 61972142), the Hunan Provincial Natural Science Foundation of China (Grant No. 2020JJ4212).

References

[1] M. C. Stamm, M. Wu, and K. J. R. Liu, "Information forensics: An overview of the first decade," *IEEE Access*, vol. 1, pp. 167–200, 2013.

[2] A. C. Popescu and H. Farid, "Exposing digital forgeries by detecting traces of resampling," *IEEE Transactions on Signal Processing*, vol. 53, pp. 758–767, Feb. 2005.

[3] X. Feng, I. J. Cox, and G. Doerr, "Normalized energy density-based forensic detection of resampled images," *IEEE Transactions on Multimedia*, vol. 14, no. 3, pp. 536–545, Jun. 2012.

[4] M. C. Stamm and K. J. R. Liu, "Forensic detection of image manipulation using statistical intrinsic fingerprints," *IEEE Transactions on Information Forensics and Security*, vol. 5, no. 3, pp. 492–506, Sep. 2010.

[5] G. Cao, Y. Zhao, R. Ni, and X. Li, "Contrast enhancement-based forensics in digital images," *IEEE Transactions on Information Forensics and Security*, vol. 9, no. 3, pp. 515–525, Mar. 2014.

[6] Y. Zhang, S. Li, S. Wang, and Y. Q. Shi, "Revealing the traces of median filtering using high-order local ternary patterns," *IEEE Signal Processing Letters*, vol. 21, no. 3, pp. 275–279, Mar. 2014.

[7] A. Peng, S. Luo, H. Zeng, and Y. Wu, "Median filtering forensics using multiple models in residual domain," *IEEE Access*, vol. 7, pp. 28 525–28 538, Feb. 2019.

[8] H. Li, W. Luo, X. Qiu, and J. Huang, "Identification of various image operations using residual-based features," *IEEE Transactions on Circuits and Systems for Video Technology*, vol. 28, no. 1, pp. 31–45, Jan. 2018.

[9] J. Chen, X. Liao, W. Wang, and Z. Qin, "A features decoupling method for multiple manipulations identification in image operation chains," in *2021 IEEE International Conference on Acoustics, Speech and Signal Processing (ICASSP)*, 2021, pp. 2505–2509.

[10] J. Chen, X. Liao, and Z. Qin, "Identifying tampering operations in image operator chains based on decision fusion," *Signal Processing: Image Communication*, vol. 95, pp. 116 287(1)–116 287(10), Jul. 2021.

[11] M. C. Stamm, X. Chu, and K. J. R. Liu, "Forensically determining the order of signal processing operations," in *2013 IEEE International Workshop on Information Forensics and Security (WIFS)*, Guangzhou, China, Nov. 2013, pp. 162–167.

[12] X. Chu, Y. Chen, and K. J. R. Liu, "An information theoretic framework for order of operations forensics," in *2016 IEEE International Conference on Acoustics, Speech and Signal Processing (ICASSP)*, Shanghai, China, Mar. 2016, pp. 2049–2053.

[13] X. Liao, K. Li, X. Zhu, and K. J. R. Liu, "Robust detection of image operator chain with two-stream convolutional neural network," *IEEE Journal of Selected Topics in Signal Processing*, vol. 14, no. 5, pp. 955–968, Aug. 2020.

[14] Y. Huang, L. Cao, J. Zhang, L. Pan, and Y. Liu, "Exploring feature coupling and model coupling for image source identification," *IEEE Transactions on Information Forensics and Security*, vol. 13, no. 12, pp. 3108–3121, Dec. 2018.

[15] B. Patrick, T. Filler, and T. Pevný, "Break our steganographic system: The ins and outs of organizing boss," in *2011 International Workshop on Information Hiding*, Berlin, Heidelberg, May 2011, pp. 59–70.

[16] G. Schaefer and M. Stich, "Ucid: an uncompressed color image database," in *Storage and Retrieval Methods and Applications for Multimedia*, San Jose, California, United States, Dec. 2003, pp. 472–481.